

# Dynamics of the Ising Spin-Glass Model in a Transverse Field

M. J. Rozenberg<sup>1</sup> and D. R. Grempel<sup>2</sup>

<sup>1</sup>*Institut Laue-Langevin, BP156, 38042 Grenoble, France*

<sup>2</sup>*Département de Recherche Fondamentale sur la Matière Condensée  
SPSMS, CEA-Grenoble, 17, rue des Martyrs, 38054 Grenoble Cedex 9, France*

(August 13, 2018)

We use quantum Monte Carlo methods and various analytic approximations to solve the Ising spin-glass model in a transverse field in the disordered phase. We focus on the behavior of the frequency dependent susceptibility of the system above and below the critical field. We establish the existence of an exact equivalence between this problem and the single-impurity Kondo model at the quantum critical point. Our predictions for the long-time dynamics of the model are in good agreement with experimental results on  $\text{LiHo}_{0.167}\text{Y}_{0.833}\text{F}_4$ .

75.10.Jm, 75.40.Gb, 75.10.Nr

The physics of frustrated quantum spin systems is a fascinating and rapidly growing area of condensed matter physics [1]. One of the most widely investigated systems is the Ising spin glass in a transverse field, a model that combines simplicity and experimental accessibility [2,3]. The Hamiltonian of the model reads,

$$H = -\frac{1}{\sqrt{N}} \sum_{i<j} J_{ij} S_i^z S_j^z - \Gamma \sum_i S_i^x, \quad (1)$$

where  $S_i^\mu$ ,  $\mu = x, z$  are components of a three dimensional spin-1/2 operator at the  $i$ -th site of a fully-connected lattice of size  $N$  and the first sum runs over all pairs of sites. The exchange interactions  $J_{ij}$  are independent random variables with a gaussian distribution of zero mean and variance  $J = \langle J_{ij}^2 \rangle^{1/2}$ , and  $\Gamma$  is an applied magnetic field transverse to the easy-axis  $z$ . For  $\Gamma = 0$  Eq. 1 is the classical Sherrington-Kirkpatrick spin-glass model that has a second order phase transition at  $T_g^0 = J/4$ . When  $\Gamma$  is finite quantum fluctuations compete with the tendency of the system to develop spin-glass order. As a result a boundary  $\Gamma(T)$  appears in the  $\Gamma - T$  plane between spin-glass (SG) and paramagnetic (PM) phases.

The model of Eq.1 is relevant for the compound  $\text{LiHo}_{0.167}\text{Y}_{0.833}\text{F}_4$ , a site-diluted derivative of the dipolar-coupled Ising ferromagnet  $\text{LiHoF}_4$  [2]. An external magnetic field  $H_t$  perpendicular to the easy axis splits the doubly degenerate ground state of the  $\text{Ho}^{3+}$  ion. This splitting is proportional to  $H_t^2$  and plays the role of  $\Gamma$  in Eq. 1 [2,4]. Experimentally,  $\text{LiHo}_{0.167}\text{Y}_{0.833}\text{F}_4$  is paramagnetic at all temperatures above a critical field  $H_t^c \approx 12$  kOe [2,3]. Below  $H_t^c$  and for  $T \gtrsim 25$  mK the behavior of the non-linear susceptibility indicates a second order transition line between SG and PM phases that ends at  $T_g^0 = 135$  mK and  $H_t = 0$  [5]. Investigation of the long-time dynamics of this system above this line has revealed the existence of a fast crossover in the field dependence of the absorption at very low frequencies [2,3]. This crossover is characterized by a steep increase of  $\chi''(\omega \rightarrow 0)$  across an almost flat line in the  $\Gamma - T$  plane at  $\Gamma \approx \Gamma_c$  and up to  $T \sim T_g^0$ .

While the phase diagram of the model has been studied theoretically using a variety of methods [8,9,10], much less is known about its dynamics that has only been discussed for large  $\Gamma/J$  [11], and near the quantum critical point [12].

In this paper we use a recently developed quantum Monte Carlo method (QMC) [13] to find the exact numerical paramagnetic solutions of the model throughout the  $\Gamma - T$  plane, and also obtain analytic expressions that we derive in various limiting cases. We find that the behavior of  $\chi''(\omega)$  above and below the critical field is qualitatively different. For  $\Gamma > \Gamma_c$  the zero-temperature spectrum of magnetic excitations has a gap  $\Delta$  [12] that vanishes as  $\Gamma \rightarrow \Gamma_c \approx 0.76J$ . At finite but low temperatures,  $T < \Delta$ , the gap edge develops a tail of exponentially small weight. On the other hand, for small  $\Gamma$  and low  $T$ , we find a narrow feature around  $\omega = 0$  whose intensity decreases rapidly with increasing field or temperature as spectral weight is transferred to higher frequencies. We further demonstrate that at the quantum critical point the problem can be exactly mapped to the single-impurity Kondo model. The low-energy properties of the system in the neighborhood of this point are characterized by a new energy-scale,  $T_0 \approx 0.08J$ . At finite temperature there is a crossover between the regimes just mentioned that is essentially controlled by  $\Gamma$  up to  $T \sim T_g^0$ . We finally present detailed predictions for the  $\Gamma$  and  $T$ -dependence of the low-frequency response that are in good agreement with the experimental results on  $\text{LiHo}_{0.167}\text{Y}_{0.833}\text{F}_4$  [3].

Bray and Moore [14] have shown that the quantum spin-glass problem can be exactly transformed into a single-spin problem with a time-dependent self-interaction  $Q(\tau)$  determined by the feedback effects of its coupling to the rest of the spins. As we have shown elsewhere for a related problem [13], much progress can be made by eliminating the self-interaction in favor of an auxiliary fluctuating time-dependent field  $\eta(\tau)$  coupled to the spins. The free-energy per site  $\mathcal{F}$  in the paramagnetic phase can then be written as

$$\beta\mathcal{F} = \min_{Q(\tau)} \left\{ \frac{J^2}{4} \int_0^\beta \int_0^\beta d\tau d\tau' Q^2(\tau - \tau') - \ln Z_{\text{loc}}[Q] \right\},$$

$$Z_{\text{loc}}[Q] = \int \mathcal{D}\eta \exp \left[ -\frac{1}{2} \int_0^\beta \int_0^\beta d\tau d\tau' Q^{-1}(\tau, \tau') \eta(\tau) \eta(\tau') \right]$$

$$\times \text{Tr} \mathcal{T} \exp \left[ \int_0^\beta d\tau [J\eta(\tau) S^z(\tau) + \Gamma S^x(\tau)] \right], \quad (2)$$

where  $\mathcal{T}$  is the time-ordering operator along the imaginary-time axis  $0 \leq \tau \leq \beta$ .  $Z_{\text{loc}}$  can be thought of as the average partition function of a spin in an effective magnetic field  $\vec{h}_{\text{eff}} = J\eta(\tau)\hat{e}_z + \Gamma\hat{e}_x$  whose  $z$ -component is a random gaussian function with variance  $Q(\tau)$ . The latter is determined by functional minimization of (2) which gives the self-consistency condition [14]

$$Q(\tau) = \langle \mathcal{T} S^z(\tau) S^z(0) \rangle_{\eta(\tau)}, \quad (3)$$

where the average is taken with respect to the probability density associated to  $Z_{\text{loc}}$ . We solved Eqs. 2-3 iteratively using the QMC technique that we have described elsewhere [13]. The imaginary time axis is discretized in up to  $L = 128$  time slices with  $\Delta\tau = \beta/L \leq 0.5$ . An iteration consists of at least 20,000 QMC steps per time-slice and self-consistency is generally attained after about eight iterations except very close to the quantum critical point. We mapped the spin-glass transition line in the  $\Gamma - T$  plane using the well known stability criterion [14]  $1 = J\chi_{\text{loc}}$  where  $\chi_{\text{loc}} = \int_0^\beta d\tau Q(\tau)$  is the local spin-susceptibility. We found a second-order transition line ending at a quantum critical point at  $T = 0$  in agreement with previous work [8,9,10]. Going down in temperature to  $T \sim 10^{-2}J$  and extrapolating the results to  $T = 0$  we determined a precise value for the critical field  $\Gamma_c/J = 0.76 \pm 0.01$ , which lies in between previous estimates [12,10].

We have studied the dynamical properties of the paramagnetic state throughout the  $\Gamma - T$  plane, even below  $T_g$  where it is unstable. Indeed, the analysis of the evolution of the paramagnetic solution for small  $\Gamma$  provides insight on the physics of this problem as the states below and above  $T_g$  are continuously connected. In Fig.1 we show the correlation function for several values of  $\Gamma$  and  $T$ . For  $\Gamma > \Gamma_c$  (panel a),  $Q(\tau)$  decays exponentially with a time-constant  $\tau_0 \approx \Gamma^{-1} \ll \beta$  that depends only weakly on  $T$ . This behavior is characteristic of the existence of a gap  $\Delta \sim \Gamma$  in the excitation spectrum of the system. For  $\Gamma < \Gamma_c$  and  $T \ll J$  (panel c),  $Q(\tau)$  also decays very rapidly for short times,  $\tau \lesssim \tau_0 \sim \beta^{-1}$ . For  $\tau \gtrsim \tau_0$ , however, it exhibits a very slow variation which indicates that the presence of excitations in the low-energy end of the spectrum,  $\omega \ll T$ . With increasing temperature  $\tau_0$  increases and reaches a value  $\mathcal{O}(J^{-1})$  when  $T \sim J$ . It then becomes no longer possible to distinguish two different time scales. The case  $\Gamma = \Gamma_c$  at low temperature (panel b) is intermediate between the other two and the

long-time behavior becomes a power-law,  $Q(\tau) \propto \tau^{-2}$  as  $T \rightarrow 0$ , as anticipated by Miller and Huse [12] using internal consistency arguments. The solid lines in Fig. 1 are the results of various analytic approximations that we discuss next. We begin by considering  $\Gamma/J \gg 1$ . In this case, the effective fields appearing in Eq. 2 are dominated by their  $x$ -component. We may thus evaluate the trace of the time-ordered exponential under the integral in  $Z_{\text{loc}}$  using a low-order cumulant expansion. To the lowest non-trivial order we find,

$$\chi''(\omega) = \frac{\text{sgn}(\omega)}{2\Gamma J m_x} \sqrt{(2\Gamma J m_x)^2 - (\omega^2 - \Gamma^2)^2}, \quad (4)$$

where  $m_x = 1/2 \tanh(\beta\Gamma/2)$  is the zero-th order transverse magnetization. Eq. 4 predicts the existence of a gap  $\Delta = \sqrt{\Gamma^2 - 2\Gamma J m_x}$  in the excitation spectrum. This gap has a very weak temperature dependence for  $T \ll \Gamma$  and, at  $T = 0$ , vanishes at  $\Gamma_c/J = 1$ , overestimating the critical field. It can be shown [15] that, for  $T \ll \Delta$ , the gap-edge develops a tail that carries a small weight  $\mathcal{O}(e^{-\Delta/T})$ .

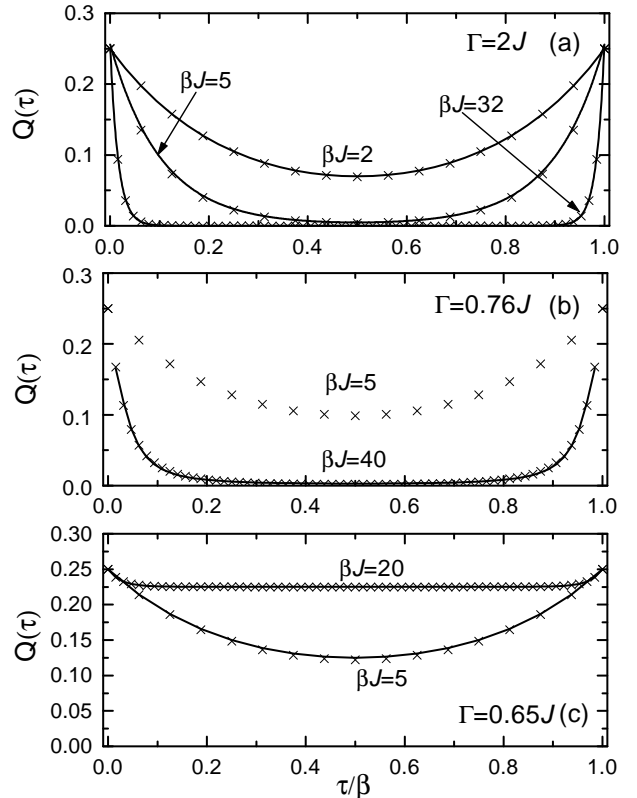


FIG. 1.  $Q(\tau)$  as function of  $\tau/\beta$ . The crosses correspond to QMC data. The error bars are smaller than the size of the crosses. The solid lines are obtained using the analytic expressions discussed in the text.

This procedure breaks down at  $\Gamma/J \sim 1$  and a different approach must be taken in order to describe the physics at low fields. At  $\Gamma = 0$ , the problem reduces to the

classical Sherrington-Kirkpatrick model and  $Q(\tau) \equiv 1/4$  at all temperatures. We thus expect that for  $\Gamma/J \ll 1$  the effective field  $\tilde{h}_{\text{eff}}(\omega_n)$  will be dominated by its  $\omega = 0$  component. Indeed, setting for the moment  $\eta(\omega) = 0$  for  $\omega \neq 0$  in Eq. 3 and performing the functional average solely over static fields  $\eta(\tau) \equiv \eta_0$ , we find

$$Q(\omega_n) = \left\langle \frac{\beta J^2 \eta_0^2 / 4}{\Gamma^2 + J^2 \eta_0^2} \right\rangle_{\eta_0} \delta_{n,0} + \left\langle \frac{\Gamma m(\eta_0) \cos \theta_x}{\omega_n^2 + \Gamma^2 + J^2 \eta_0^2} \right\rangle_{\eta_0}, \quad (5)$$

where  $m(\eta_0) = 1/2 \tanh(\beta \sqrt{\Gamma^2 + J^2 \eta_0^2} / 2)$  and  $\cos \theta_x = \Gamma / \sqrt{\Gamma^2 + J^2 \eta_0^2}$ . The average is performed with respect to the probability distribution,  $\mathcal{P}(\eta_0) \propto \exp(-\beta \eta_0^2 / 2 \chi_{\text{loc}}) \cosh(\beta \sqrt{\Gamma^2 + J^2 \eta_0^2} / 2)$ . Using Eqs. 2 and 5 we can deduce the region of validity of this ansatz from the estimates  $|\eta(\omega_n) / \eta(0)| \sim 32 \Gamma T^2 / J^3$  for  $T \ll J$ , and  $\sim \Gamma / (2\pi n T)$  when  $T \gg J$ . Within this approximation, the imaginary part of the response on the real axis is given by,

$$\begin{aligned} \frac{\chi''(\omega)}{\pi \omega} &= \left\langle \frac{\beta J^2 \eta_0^2 / 4}{\Gamma^2 + J^2 \eta_0^2} \right\rangle_{\eta_0} \delta(\omega) + \\ &\frac{\Gamma^2}{2\omega^2} \frac{\tanh(\beta |\omega| / 2) \mathcal{P}(\sqrt{\omega^2 - \Gamma^2})}{\sqrt{\omega^2 - \Gamma^2}}. \end{aligned} \quad (6)$$

In this regime the relaxation function  $\chi''(\omega) / \omega$  splits into two contributions, an elastic peak at  $\omega = 0$  and a continuum starting at  $\omega = \Gamma$ . The fraction of spectral weight contained in each of these two contributions is determined by the transverse field and the temperature. Evaluating the coefficient of the  $\delta$ -function in Eq. 6 we find that the relative intensity of the central peak varies between  $1 - (8\Gamma T / J^2)^2$  for  $T \ll J$ , and  $J^2 / (4\Gamma^2 + J^2)$  for  $T \gg J$ . The low-energy states represented by the  $\delta$ -function are responsible for the slow decay observed in the long-time behavior of  $Q(\tau)$  at low  $T$  in Fig.1c. The fact that the central peak has zero width is a shortcoming of the approximation leading to Eq. 5 as it does not capture the slow relaxational processes which broaden it [13]. Nevertheless, the excellent agreement between the numerical and analytic results indicates that the width of the central peak must be, in any case, much smaller than the temperature. The high-energy states described by the inelastic part of the response control the exponential decay observed for short times. The decay rate predicted by Eq. 6 is  $\tau_0^{-1} \sim J^2 \beta / 8$  for  $T \ll J$ , and  $\tau_0^{-1} \sim J$  for  $T \gg J$  in agreement with the numerical results.

The approximations discussed above can not be used near  $\Gamma = \Gamma_c$ . However, one can still gain insight on the dynamics in the critical region by exploiting an interesting analogy between the model (1) at the quantum critical point and the single impurity Kondo problem that we establish next. We first perform a Trotter decomposition of the time ordered exponential in Eq. 2 and introduce intermediate states  $|\sigma\rangle\langle\sigma|$  at each imaginary time-slice  $\tau$ . The trace is now evaluated using the expression

$$\langle \sigma | e^{\Delta\tau \tilde{h}_{\text{eff}}(\tau) \cdot \vec{S}} | \sigma' \rangle \approx e^{\Delta\tau J \eta(\tau) \sigma} \left( \delta_{\sigma\sigma'} + \delta_{\sigma\bar{\sigma}'} \frac{\Gamma \Delta\tau}{2} + \mathcal{O}(\Delta\tau^2) \right), \quad (7)$$

valid in the limit when the width of the time slice  $\Delta\tau \rightarrow 0$ . The partition function can then be expressed in terms of a sum over “histories”, each of them defined by a particular sequence of the eigenvalues  $\sigma^z(\tau) = \pm 1/2$  of the intermediate states. Going over to the continuum limit and performing the gaussian integral over the auxiliary fields  $\eta(\tau)$ , we obtain

$$\begin{aligned} Z_{\text{loc}} &= \int \mathcal{D}\sigma^z \exp \left[ \frac{J^2}{2} \int_0^\beta \int_0^\beta d\tau d\tau' \sigma^z(\tau) Q(\tau - \tau') \sigma^z(\tau') \right. \\ &\quad \left. + \ln(\Gamma/2) \times (\text{number of spin flips}) \right], \end{aligned} \quad (8)$$

where by “number of spin flips” we mean the number of times that the function  $\sigma^z(\tau)$  changes sign in the interval  $0 \leq \tau \leq \beta$ . This expression has a form analogous to that of the partition function of the single-impurity Kondo model in the Anderson-Yuval formalism [16]. In Eq. 8,  $\Gamma$  and  $J^2 Q(\tau)$  play the roles of the spin-flip coupling  $J_\pm$  and the long-range Ising-like effective interaction in the Kondo model [16]. Still, there is an important difference between the two problems. In the latter the Ising-like interaction is given, and behaves as  $(2 - \epsilon) / \tau^2$  with  $\epsilon \propto J_z$  as  $T \rightarrow 0$  [16]. When the dynamics of the impurity-spin is controlled by the strong-coupling fixed point, its time-dependent correlation function is also  $\propto \tau^{-2}$  at long times. In contrast, in our problem,  $Q(\tau)$  is *a priori* unknown. However, one realizes that, if for some  $\Gamma$  the asymptotic behavior of  $Q(\tau)$  is  $\sim \tau^{-2}$  then, by virtue of (8) and the identifications just made, the two problems become equivalent at that value of the field and  $T = 0$ . This is indeed the case at  $\Gamma_c$  where, as shown in Fig. 1b, the self-consistent solution of the problem at low  $T$  can be accurately fitted by the finite-temperature generalization of Anderson and Yuval’s Ising-like interaction [16] using  $\tau_0 \sim \Gamma_c^{-1}$  as a short-time cutoff. This analogy between our problem and the Kondo model provides a simple way to estimate the energy-scale associated with the low-energy excitations at the quantum critical point. It is well known [17] that the local susceptibility of the Kondo impurity is given by  $T_0 \chi_{\text{loc}}(T) = \phi(T/T_0)$ , where  $\phi$  is a universal function with  $\phi(0) \approx 0.0796$  [17] and  $T_0$  is the Kondo scale. Since in our case  $\chi_{\text{loc}} = J^{-1}$  at the quantum critical point, it follows that  $T_0 \approx 0.0796 J$ . We expect the quantum critical region to extend up to a temperature  $T_{\text{qc}}$  of this order. Our detailed numerical results for the temperature dependence of the local susceptibility are consistent with  $T_{\text{qc}} \sim T_0 / 4$  [15].

Finally, we would like to discuss the experimentally observed crossover dynamics in  $\text{LiHo}_{0.167}\text{Y}_{0.833}\text{F}_4$  in the light of the results presented here. By measuring the response of the system at 1.5 Hz, the experiment [3] is

probing the intensity of the low-lying excitations represented by the  $\delta$ -function peak in Eq. 6.

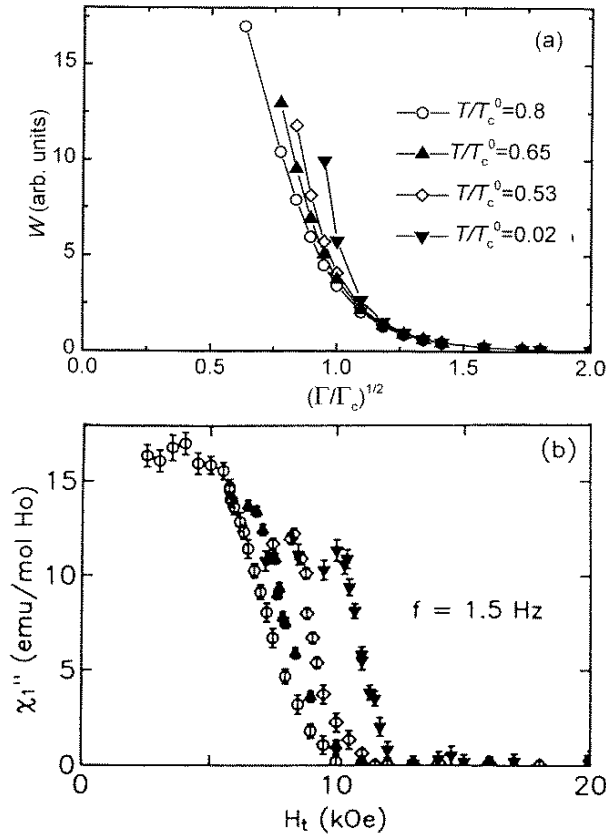


FIG. 2. (a) Spectral weight of the central peak in Eq. 6 as a function of  $(\Gamma/\Gamma_c)^{1/2}$  for several temperatures. (b) Imaginary part of the linear susceptibility of  $\text{LiHo}_{0.167}\text{Y}_{0.833}\text{F}_4$  at 1.5 Hz as a function of  $H_t$ . Data correspond to  $T=98, 82, 66$  and 25 mK, from left to right. From Ref. [3]

In Fig. 2 we compare the intensity of the latter (upper panel) and the experimental data of Ref. [3] (lower panel) at various temperatures. To make the connection with the experiment we plot the theoretical results as a function of  $(\Gamma/\Gamma_c)^{1/2}$  since the splitting of the ground-state doublet of the  $\text{Ho}^{3+}$  ion is proportional to the square of  $H_t$ . The temperatures chosen for our calculations are such that the ratios  $T/T_g^0$  correspond to the experimental values. There are no free parameters other than the overall scale of the  $y$ -axis. The theoretical curves end at the field  $\Gamma_c(T)$  where the condition  $J\chi_{loc} = 1$  is fulfilled. For lower fields, the system enters the spin-glass phase and the experimental data become field-independent. As the figure demonstrates the overall behavior of the theoretical curves is in remarkable agreement with the experiment. Two important features are worth noticing. Firstly, the value of the field at the onset of absorption,  $H_t \approx H_t^c$  is almost temperature-independent which explains the flatness of the experimental crossover line. Secondly, for  $T \sim T_g^0$ , absorption starts well above  $\Gamma_c(T)$ ,

meaning that precursor low-lying excitations appear in the paramagnetic phase long before the system freezes.

In conclusion, we have presented an exact numerical solution of the infinite-range Ising spin-glass model in a transverse field in the paramagnetic phase. We worked out analytic approximations in different limiting cases that allow for a physical interpretation of the numerical data. In particular, we established for the first time an interesting connection between this problem and the single-impurity Kondo model. Our prediction for dynamics of the model are in good agreement with experimental results on  $\text{LiHo}_{0.167}\text{Y}_{0.833}\text{F}_4$ .

- 
- [1] D. S. Fisher, Phys. Rev. Lett. **69**, 534 (1992); Phys. Rev. B **51**, 6411 (1995). N. Read, S. Sachdev and J. Ye, Phys. Rev. B **52**, 384 (1995). H. Rieger und A. P. Young, *Quantum Spin Glasses*, Lecture Notes in Physics **492** "Complex Behavior of Glassy Systems", p. 254, ed. J.M. Rubi and C. Perez-Vicente (Springer Verlag, Berlin-Heidelberg-New York, 1997).
  - [2] W. Wu, B. Ellman, T. F. Rosenbaum, G. Aeppli and D. H. Reich, Phys. Rev. Lett. **67**, 2076 (1991).
  - [3] W. Wu, D. Bitko, T. F. Rosenbaum and G. Aeppli, Phys. Rev. Lett. **71**, 1919 (1993).
  - [4] P. E. Hansen, T. Johansson and R. Nevald, Phys. Rev. B **12**, 5315 (1975).
  - [5] There is some indication [3] that the phase transition might become first-order below 25 mK, a puzzling result [6,7] that we do not discuss in this paper.
  - [6] J. Mattsson, Phys. Rev. Lett. **75**, 1678 (1995).
  - [7] W. Wu, D. Bitko, T. F. Rosenbaum and G. Aeppli, Phys. Rev. Lett. **75**, 1679 (1995).
  - [8] K. D. Usadel, Solid State Commun. **58**, 629 (1986).
  - [9] T. Yamamoto and H. Ishii, J. Phys. C **20**, 6053 (1987).
  - [10] Y. Y. Goldschmidt and P. Y. Lai, Phys. Rev. Lett. **64**, 2467 (1990).
  - [11] Y. V. Fedorov and E. F. Shender, Pis'ma Zh. Exsp. Teor. Fiz. **43**, 526 (1986) [JETP Lett. **43**, 681 (1986)].
  - [12] J. Miller and D. A. Huse, Phys. Rev. Lett. **70**, 3147 (1993).
  - [13] D. R. Grempel and M. J. Rozenberg, Phys. Rev. Lett. **80**, 389 (1998).
  - [14] A. J. Bray and M. A. Moore, J. Phys. C **13**, L655 (1980).
  - [15] D. R. Grempel and M. J. Rozenberg (unpublished).
  - [16] P. W. Anderson and G. Yuval, Phys. Rev. Lett. **23**, 89 (1969). P. W. Anderson, G. Yuval and D. R. Hammann, Phys. Rev. B **1**, 4464 (1970).
  - [17] H. R. Krishna-murthy, K. G. Wilson and J. W. Wilkins, Phys. Rev. Lett. **35** 1101 (1975). A. J. Jerez (private communication).